(2)

FINAL REPORT
(March 1, 1986 – February 29, 1988)

Grantee: The Regents of the University of Colorado, Boulder, CO 80309

Grant Title: Stratospheric Constituent Response to Vertically Propagating Equatorial Waves

Principal Investigator: Murry L. Salby
Associate Professor
Department of Astrophysical, Planetary, and Atmospheric Sciences
Boulder, CO 80309

Grant Numbers: ONR Grant No. N00014-86-K-0151
University of Colorado No. 1533110

1. Introduction

Planetary-scale equatorial waves play an important role in the dynamics of the tropical atmosphere. For some time, Kelvin and mixed Rossby-gravity waves have been identified as the sources of westerly and easterly momentum for the quasi-biennial oscillation (Lindzen and Holton, 1968; Holton and Lindzen, 1972)in zonal wind, which prevails in the lower stratosphere. These large-scale disturbances were first discovered in radiosonde observations (Wallace and Kousky, 1968; Yanai and Murakami, 1970). They are believed to be excited in unsteady convective heating in the tropical troposphere. From convective centers in the intertropical convergence zone (ITCZ), equatorial waves propagate vertically into the upper atmosphere where they are eventually absorbed, e.g., through radiative dissipation.

The first global picture of equatorial waves emerged from limb-viewing satellite observations (Salby et al., 1984), revealing a spectrum of vertically propagating Kelvin waves. Trapped about the equator, these waves were seen to radiate vertically out of the tropical troposphere. In addition to the Wallace and Kousky variety, two other Kelvin waves were found. A disturbance first reported by Hirota (1978) with roughly twice the phase speed of the Wallace and Kousky wave was present. Faster by nearly a factor of four over the Wallace and Kousky wave and a factor of two over the Hirota wave was the ultrafast Kelvin wave, moving at nearly 120 m/s and seen to propagate to the highest altitude observed by Nimbus-7 LIMS. Although these three classes of Kelvin waves differ in phase speed, vertical structure, and lateral scale, each has the form of a Kelvin wave, a Gaussian centered on the equator and propagating vertically, and all satisfy the dispersion relationship for equatorial Kelvin waves.

These vertically propagating Kelvin waves account for a substantial fraction of the temperature variability in the tropical stratosphere. In combination, they lead to temperature fluctuations in excess of 5K in the upper stratosphere and mesosphere. Because several chemical constituents are photochemically controlled in this region, vertically propagating Kelvin waves are expected to lead to variations in the abundances of such species. Through temperature sensitivity of their chemical rate coefficients, several species should respond photochemically to the fluctuating wave field. At lower altitudes, where species are under dynamical control, equatorial waves may modify constituent distributions through vertical advection. This investigation explores the behavior of stratospheric species, observed by satellite, and their connection to vertically propagating equatorial waves.

2. Research effort

Distributions of ozone, nitrous oxide, and nitric acid in the stratosphere are available from LIMS retrievals over the period in which temperature variability was studied by Salby et al. (1984). The methods used in that study to isolate Kelvin wave activity in temperature variability was applied to LIMS data in hopes of identifying the signature of these disturbances in species of short photochemical lifetime.

A difficulty arose in applying the procedure to these data. The original study of temperature variability was carried out with LIMS Version 4 (V4) data, retrieved and mapped with a particular scheme. However, in the interim, the data were reprocessed with a different scheme, resulting in Version 5 (V5), which was eventually adopted as the archival product. Although this subsequent processing led to a number of improvements, equatorial wave activity was adversely affected by changes in retrieval and mapping (Hitchman, 1985; Hitchman and Leovy, 1986). Much of the Kelvin wave activity identified originally in LIMS V4 was eliminated. The weaker equatorial wave activity present in the V5 data has been attributed to poorer vertical resolution inherent to the scheme used to process those data.

Our initial investigation with the V5 data did exhibit Kelvin wave activity in the tropical temperature field. However, signals of this activity were substantially lower than that originally deduced with the V4 data. Moreover, the discrepancy does not appear to be ascribable solely to vertical resolution. There is a clear elimination of higher frequencies, *irrespective of vertical scale*. These components have the *longest* vertical wavelengths, making them most easily observed. Hence, if lower frequency components of shorter vertical wavelength can be resolved, these high frequency components should be even better resolved in the vertical scan. The elimination of higher frequency components points to some element of the processing which acts expressly to the temporal behavior. The Kalman filtering scheme used to synoptically map the data is a likely candidate. By operating this scheme with different parameters, which control how rapidly variations may occur (these parameters are more or less ad hoc, selected independently of the data), different frequencies could be admitted between the V4 and V5 data sets.

To circumvent this difficulty, it was necessary to locate and transfer the LIMS V4 data. This turned out to be a nontrivial task, as no permanent form of this data was ever archived. After some time and effort, the entire V4 data set was located, transferred, and decoded. The analysis was carried out on this archive on temperature first to ensure identity with the results obtained earlier in Salby et al., (1984). Once this had been verified, a variety of spectral analyses were carried out on ozone, nitrous oxide (ascending and descending nodes), and nitric acid.

Space-time spectral analyses were performed on the data covering the entire LIMS mission. These were broken down into frequency spectra of individual wavenumbers, each a function of latitude and height. Because wave amplitudes represent a complex time series, frequency spectra derived from these indicate both eastward and westward propagation. These spectra were examined for discrete spectral features, discriminated through vertical scale selection by the tropical forcing (Salby and Garcia, 1987). Such features were first identified in temperature, as in the original investigation (Salby et al., 1984) and then searched for in spectra of O_3, NO_2, and HNO_3. Once isolated in frequency, structures of the oscillations were composited by band-passing the variance over a range of frequencies for individual wavenumbers, each as a function of latitude and height.

3. Results

Signatures of vertically propagating Kelvin wave activity were found in temperature, O_3, NO_2 (day and night crossings), and to a lesser degree in HNO_3. Because of the volume of data involved, only a representative sample of these findings is presented here, the results of this observational study to be published in the scientific literature (Salby et al., 1988).

Fig. 1 shows power spectrum of temperature for wavenumber 2 for January–February, 1979, as a function of frequency and altitude over the equator. The data have been subjected to a Hamming window (tantamount to a 1-2-1 frequency smoothing), a 1-2-1 latitudinal smoothing, and have been decomposed into components symmetric and antisymmetric about the equator. A high-pass filter has also been applied to remove the time-mean component and effects of quasi-stationary planetary waves impinging from high latitudes. Eastward propagation (located at negative frequencies) dominates temperature variability over the equator. Much of the power is concentrated in two (and to a lesser degree three) peaks in the frequency spectrum. The dominant peak, seen to extend out of the tropical troposphere (100 mb being the lowest level) corresponds to a period of approximately 7 days and eastward propagation with a phase speed of 30 m/s. These spectra are virtually identical to those discussed in Salby et al. (1984).

Temperature power and phase corresponding to the aforementioned peak are shown as functions of latitude and height in Fig. 2. In this presentation, components symmetric about the equator are located at positive latitudes and those antisymmetric about the equator at negative latitudes. Virtually all of the temperature variance associated with this disturbance is captured by the even component (i.e., the oscillation is nearly symmetric about the equator), maximizing on the equator and falling off monotonically with latitude. The phase structure is independent of latitude, varying systematically with altitude and having a vertical wavelength of approximately 20 km. This phase behavior indicates vertical propagation only, with downward phase progression, corresponding to an upward propagation of wave activity.

Fig. 3 shows the power spectrum of O_3 for wavenumber 2 over the equator as a function of frequency and altitude. Nearly coincident with the spectral features in temperature are concentrations of ozone variability. In particular, there is a clear concentration of variance at the same frequency as the prevailing spectral peak in temperature (Fig. 1). However, this peak occurs at lower altitude than the corresponding peak in temperature, reflecting the distribution of ozone and the role of photochemistry.

That this ozone variability is indeed a consequence of Kelvin waves is demonstrated in Fig. 4, showing the latitude-height structure of the variance band-passed in this range. in the same format as Fig. 2. As is true for temperature, ozone power is chiefly symmetric about the equator. A maximum amplitude of the ozone oscillation is achieved on the equator, falling off monotonically with latitude. In altitude, the strongest oscillation occurs in the middle stratosphere, mirroring the distribution of O_3 mixing ratio. Phase behavior is also similar to that of the temperature oscillation. Above the maximum amplitude near 7 mb, there is a systematic vertical phase tilt, similar to that evident in temperature (Fig. 2). Below 10 mb, the oscillation is nearly barotropic, separated from the regular phase tilt above by a 180° phase shift. These regions of differing phase behavior correspond to altitudes where ozone is under dynamical and photochemical control respectively.

The power spectrum of NO_2 dayside data for wavenumber 2 is shown in Fig. 5 as a function of frequency and altitude. A clear peak in variance is again seen at eastward frequencies, coincident with spectral peaks in temperature. Maximum amplitudes are achieved in the middle stratosphere, as is true of the distribution of NO_2. In both O_3

and NO_2, the very lowest frequency Kelvin wave seems to lead to a stronger constituent oscillation than that at very high frequency.

Power and phase structures corresponding to the dominant peak in NO_2 are shown in Fig. 6. As before, the oscillation occurs in phase across the equator. There, the amplitude of the oscillation in NO_2 maximizes, falling off monotonically with latitude, as in the classical Kelvin wave structure and observed temperature variability. (Note: the highest altitude for which NO_2 is retrieved is 3.0 mb.) A regular phase tilt with altitude is evident across this region, as was true of temperature and ozone. However, a somewhat longer vertical wavelength than that of ozone at higher altitudes is indicated.

The behavior of HNO_3 is not as clearly identifiable with Kelvin wave temperature fluctuations. This is primarily due to variability over the equator being to a large extent confined to a neighborhood of the tropopause. The tropical tropopause is also the region where LIMS retrievals are most contaminated by clouds. The power spectrum of wavenumber 2 over the equator as a function of frequency and altitude is shown in Fig. 7. A number of peaks are evident at the lowest level (100 mb), but these quickly decay with altitude, leaving modest peaks by comparison. Nevertheless, there remains evidence of the prevailing Kelvin wave peak at eastward periods of about 7 days.

The structure of this component of HNO_3 variability (Fig. 8) is symmetric about the equator with a single maximum at zero latitude, as was true of signatures in temperature and other species. However, the latitudinal extent of the disturbance is considerably narrower that those of O_3 and NO_2. Although a systematic downward increase of phase is evident, it corresponds to a longer vertical wavelength than in any of the other quantities (except O_3 in the lower stratosphere.) Whether these discrepancies are real or artifacts of the processing is unclear at this time.

4. Future work

A clear signature of Kelvin wave activity in ozone and nitrous oxide, and to a lesser degree in nitric acid, has been found. These variations are an important component of constituent variability in the tropical stratosphere because they are identifiable in terms of dynamical fluctuations of known origin and because they represent *a significant fraction* of the variability over the equator.

Several facets of the problem remain to be explored. The structure and phasing of the constituent oscillations need to be understood. In particular, how photochemistry and the distributions of chemical species figure in determining the constituent response to vertically propagating Kelvin waves is under study (Solomon et al., 1988). It would also be valuable to understand the origin of the behavior of HNO_3, e.g., its distinction from that of other species. As additional constituents become available in future satellite observations, it will be possible to address these and other questions.

5. References

Hirota, I., 1978: Equatorial waves in the upper stratosphere and mesosphere in relation to the semi-annual oscillation in the zonal wind. *J. Atmos. Sci.*, **35**, 714.

Hitchman, M., 1985: An observational study of wave-mean flow interaction in the equatorial middle atmosphere. Ph. D. dissertation, University of Washington, 360pp.

___________, and C. Leovy, 1986: Evolution of the zonal-mean state in the equatorial middle atmosphere during October 1978–May 1979. *J. Atmos. Sci.*, **43**, 3159.

Holton, J. and R. Lindzen, 1972: An updated theory for the quasi-biennial oscillation of the tropical stratosphere. *J. Atmos. Sci.*, **29**, 1076.

Lindzen, R. and J. Holton, 1968: A theory of the quasi-biennial oscillation *J. Atmos. Sci.*, **25**, 1095.

Salby, M., D. Hartmann, P. Bailey, and J. Gille, 1984: Evidence for equatorial Kelvin modes in Nimbus-7 LIMS. *J. Atmos. Sci.*, **41**, 220.

_________, and R. Garcia, 1987: Transient response to localized episodic heating in the tropics. Part I: Short-time near-field response. *J. Atmos. Sci.*, ______.

_________, P. Callaghan, and S. Solomon, 1988: Stratospheric constituent response to vertically propagating Kelvin waves. Part I: Observations. (in preparation).

Solomon, S., P. Callaghan, and M. Salby, 1988: Stratospheric constituent response to vertically propagating Kelvin waves. Part II: Theory. (in preparation).

Yanai and Murakami, 1970: Spectrum analysis of symmetric and antisymmetric equatorial waves. *J. Meteor. Soc. Japan*, **48**, 331.

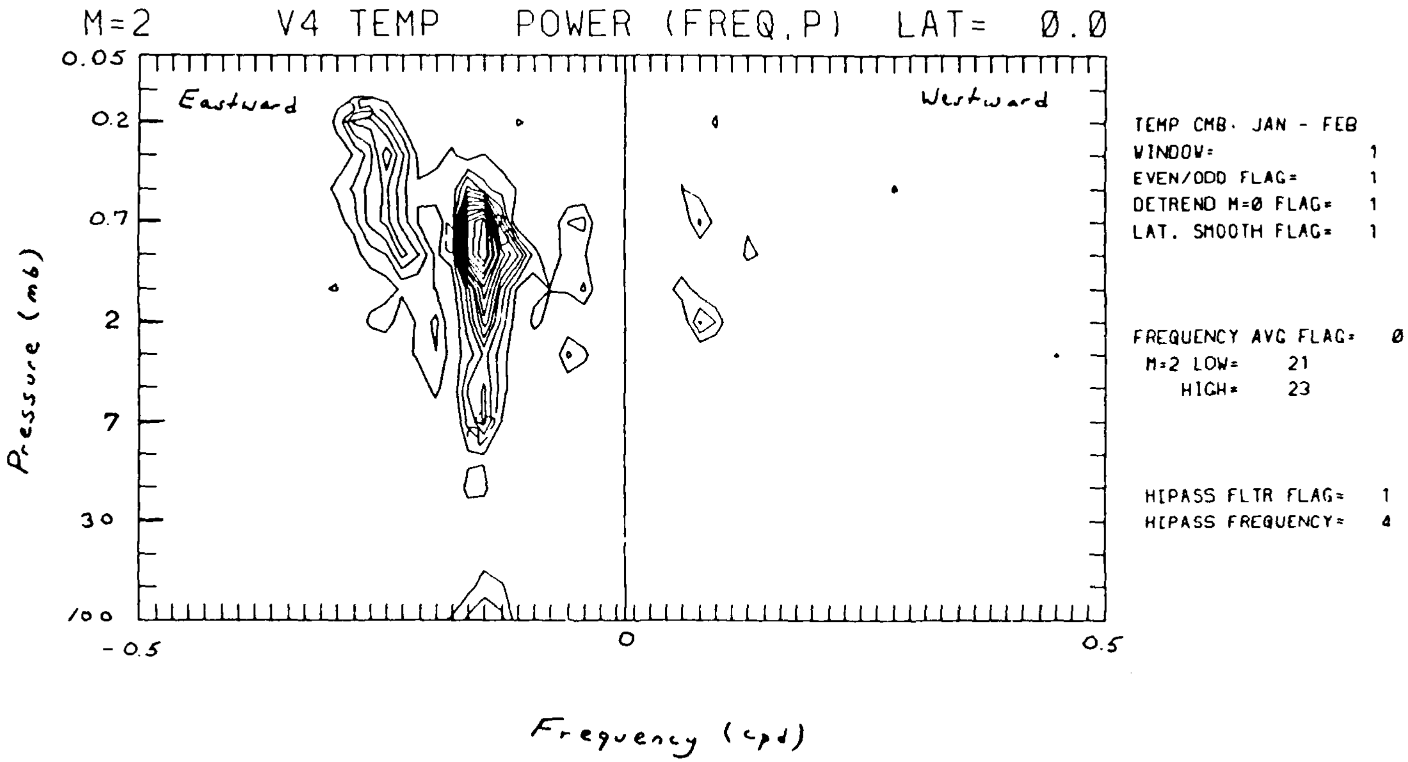

Figure 1 Temperature power as function of frequency (cpd) and pressure (mb) for wavenumber 2 over the equator during January – February 1979.

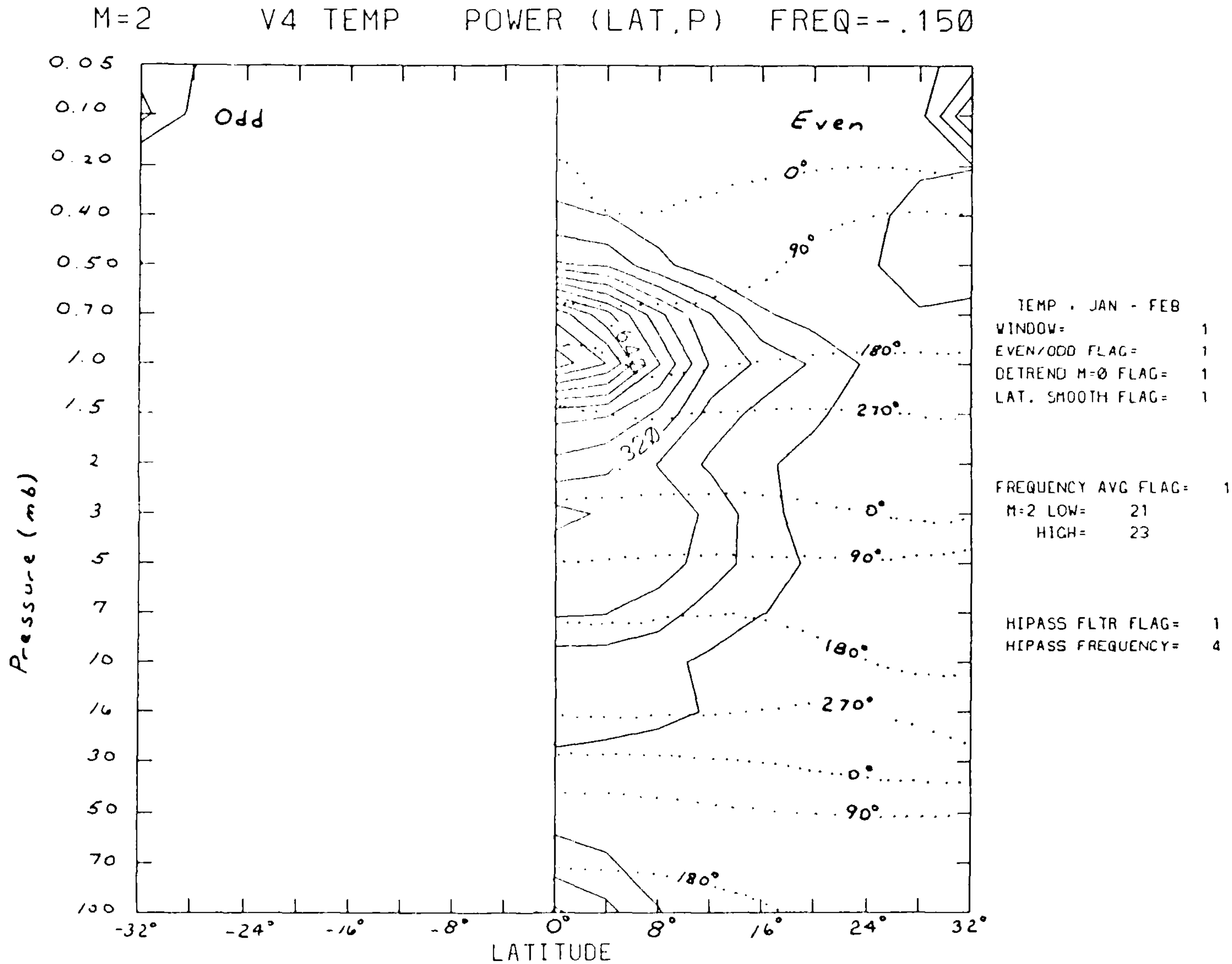

Figure 2 Temperature power (solid) and phase (dotted), band passed over eastward periods between 5.8 and 7.3 days. Varability operating symmetrically (antisymmetrically) about the equator displayed at positive (negative) latitudes. Phase structure indicates vertical propagation only, with a vertical

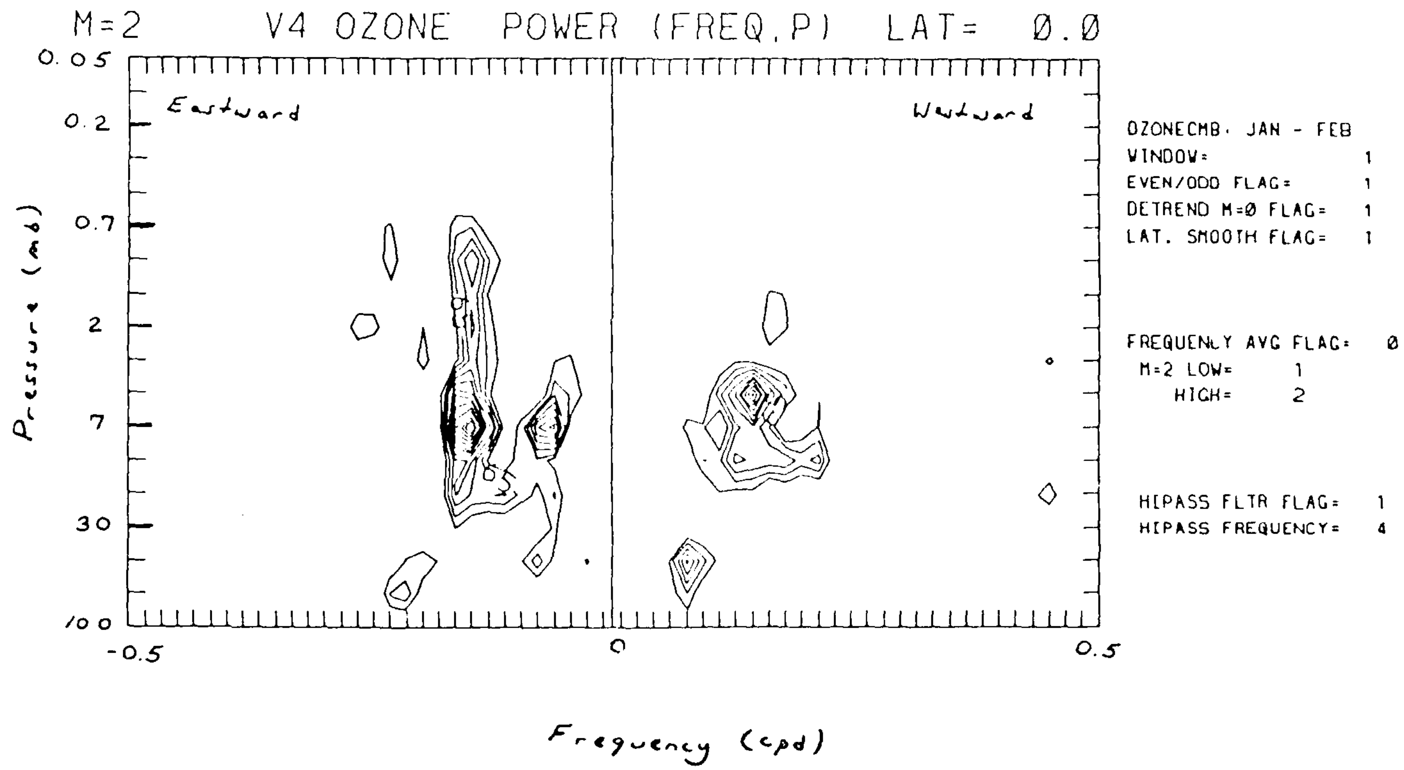

Figure 3 As for Figure 1, except for ozone.

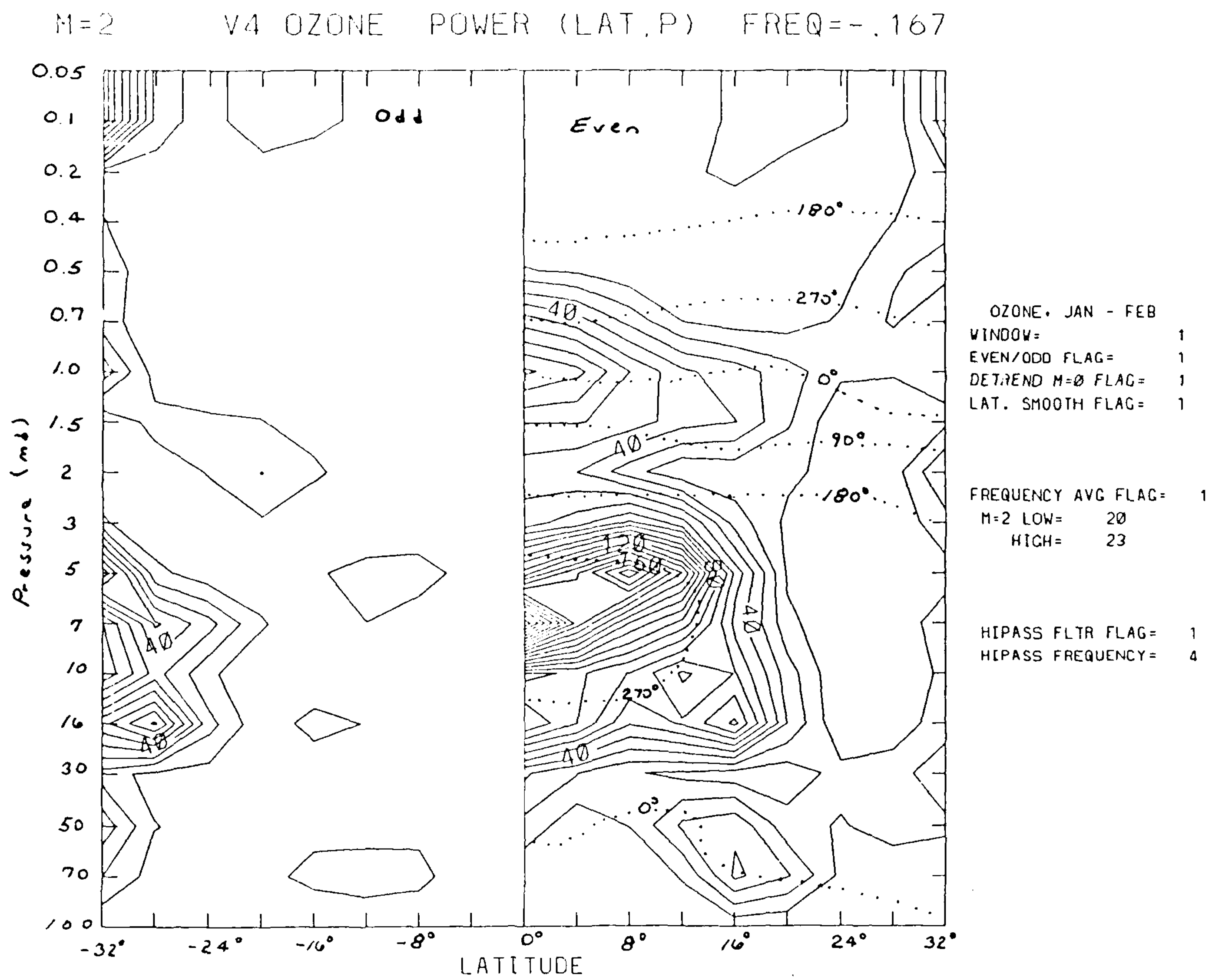

Figure 4 As for Figure 2, except for ozone.

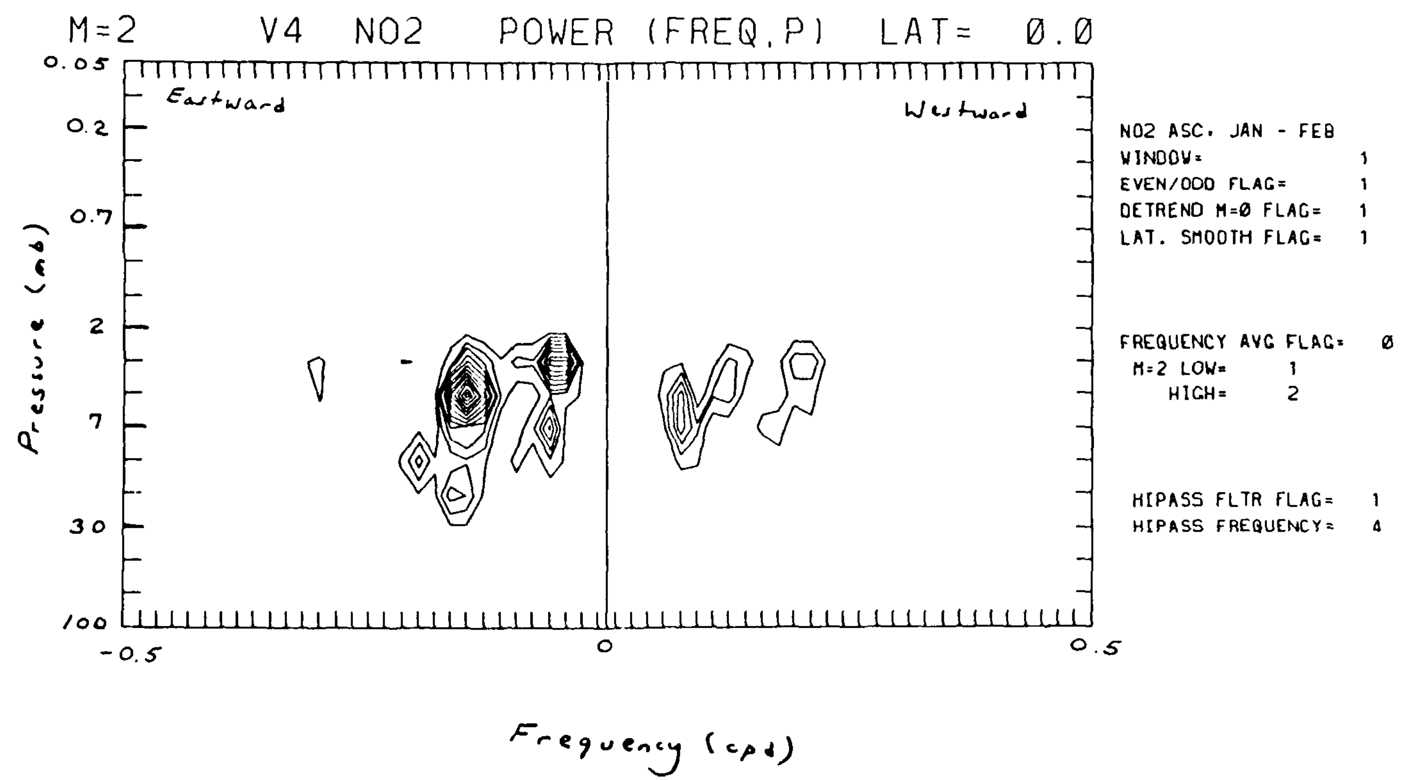

Figure 5 As for Figure 1, except for NO_2 (dayside data).

JBIRBOM Ø.ØØØØØE+ØØ TO Ø.78ØØØE-Ø3 CONTOUR INTERVAL OF

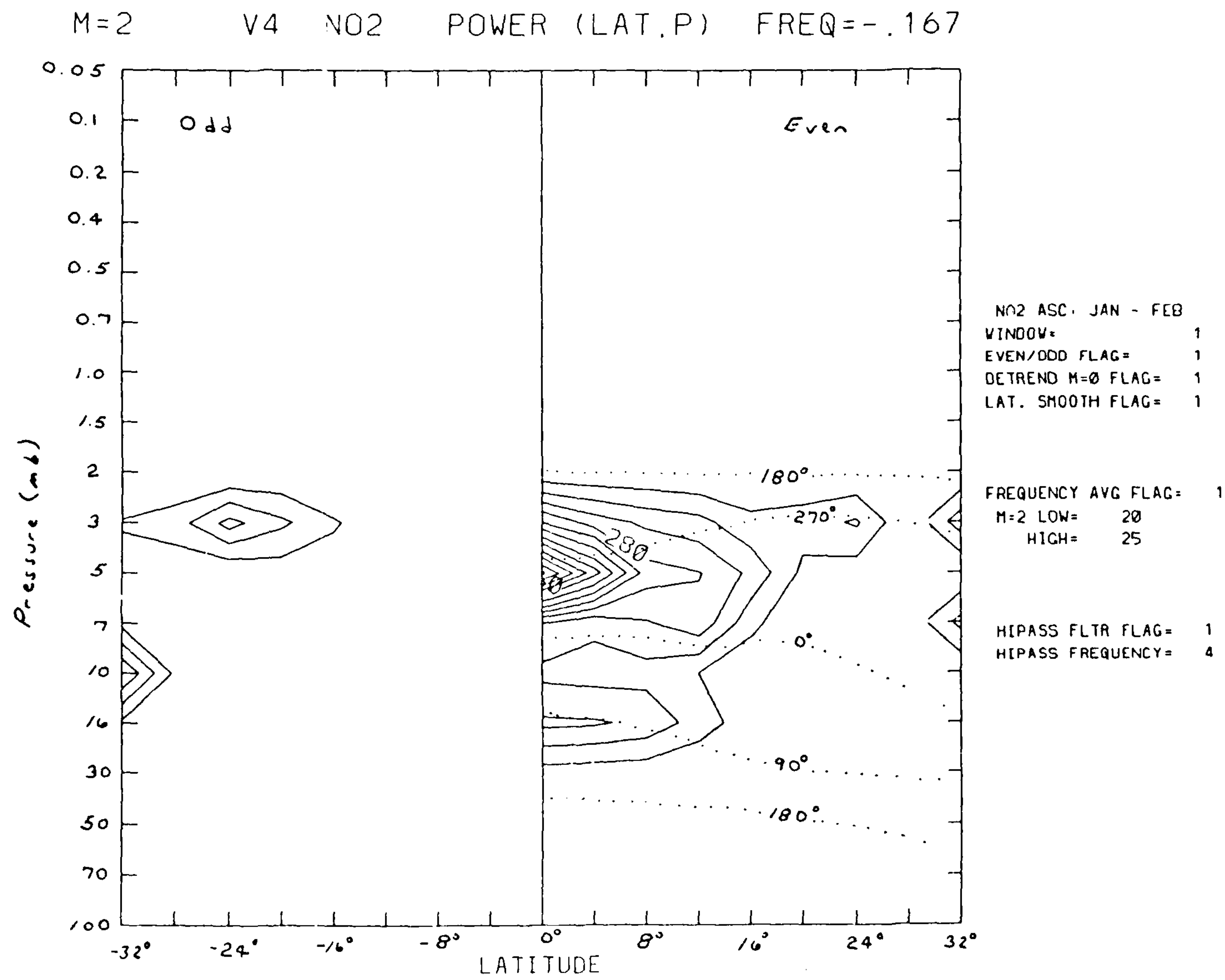

Figure 6 As for Figure 2, except for NO_2.

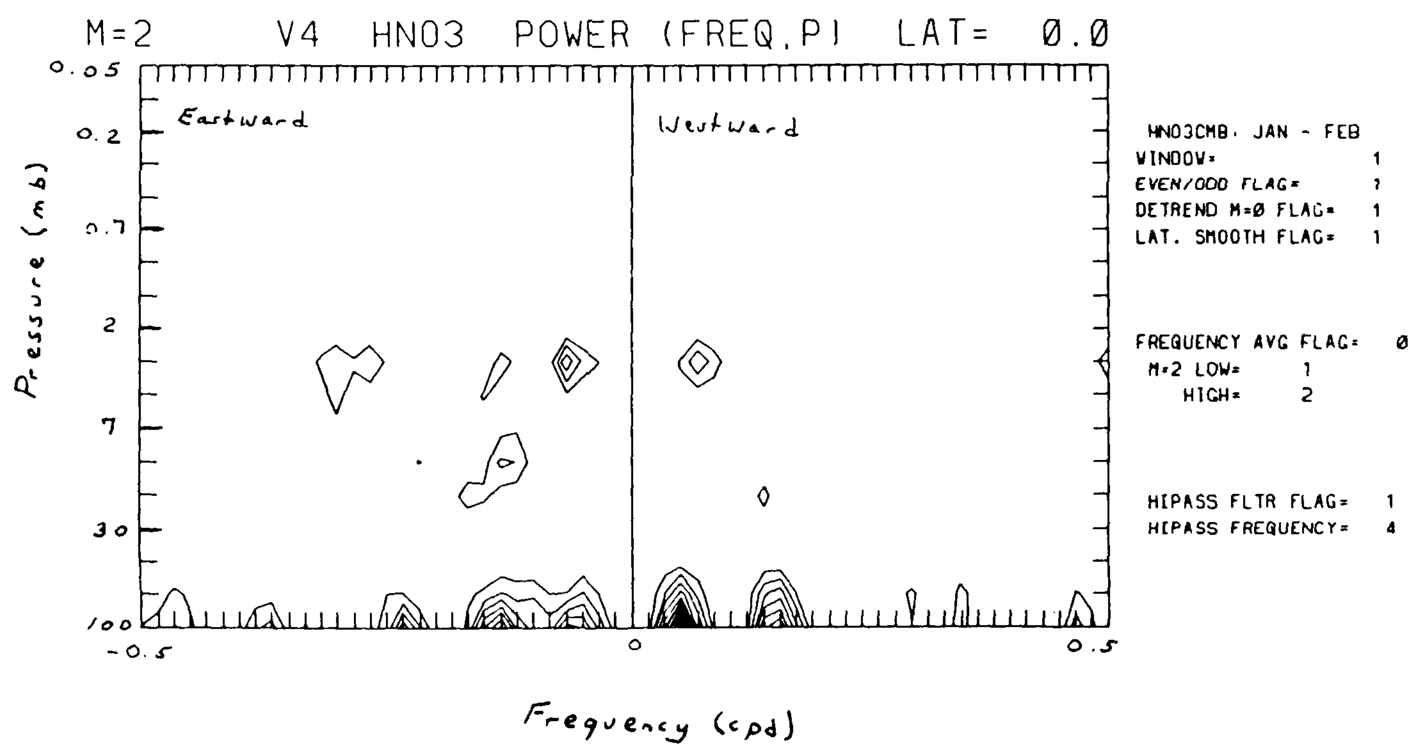

Figure 7 As for Figure 1, except for HNO_3.

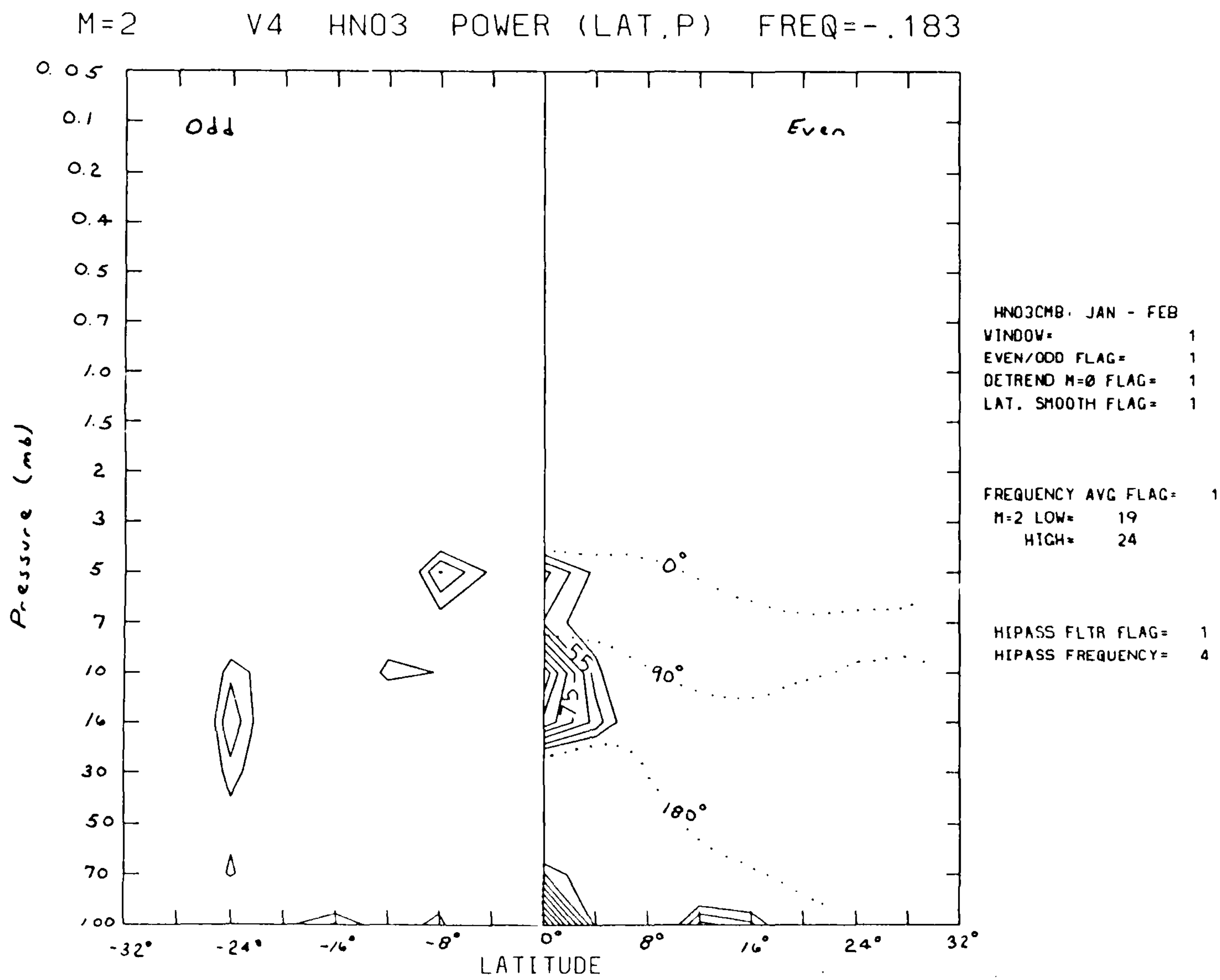

Figure 8 As for Figure 2, except for HNO_3.